JAMA Psychiatry | Original Investigation

Characterizing Heterogeneity in Neuroimaging, Cognition, Clinical Symptoms, and Genetics Among Patients With Late-Life Depression

Junhao Wen, PhD; Cynthia H. Y. Fu, MD, PhD; Duygu Tosun, PhD; Yogasudha Veturi, PhD; Zhijian Yang, MS; Ahmed Abdulkadir, PhD; Elizabeth Mamourian, MS; Dhivya Srinivasan, MS; Ioanna Skampardoni, MS; Ashish Singh, MS; Hema Nawani, PhD; Jingxuan Bao, MS; Guray Erus, PhD; Haochang Shou, PhD; Mohamad Habes, PhD; Jimit Doshi, MS; Erdem Varol, PhD; R. Scott Mackin, PhD; Aristeidis Sotiras, PhD; Yong Fan, PhD; Andrew J. Saykin, PhD; Yvette I. Sheline, MD, PhD; Li Shen, PhD; Marylyn D. Ritchie, PhD; David A. Wolk, MD, PhD; Marilyn Albert, PhD; Susan M. Resnick, PhD; Christos Davatzikos, PhD; for the iSTAGING consortium, ADNI, BIOCARD, and BLSA

IMPORTANCE Late-life depression (LLD) is characterized by considerable heterogeneity in clinical manifestation. Unraveling such heterogeneity might aid in elucidating etiological mechanisms and support precision and individualized medicine.

OBJECTIVE To cross-sectionally and longitudinally delineate disease-related heterogeneity in LLD associated with neuroanatomy, cognitive functioning, clinical symptoms, and genetic profiles.

DESIGN, SETTING, AND PARTICIPANTS The Imaging-Based Coordinate System for Aging and Neurodegenerative Diseases (iSTAGING) study is an international multicenter consortium investigating brain aging in pooled and harmonized data from 13 studies with more than 35 000 participants, including a subset of individuals with major depressive disorder. Multimodal data from a multicenter sample (N = 996), including neuroimaging, neurocognitive assessments, and genetics, were analyzed in this study. A semisupervised clustering method (heterogeneity through discriminative analysis) was applied to regional gray matter (GM) brain volumes to derive dimensional representations. Data were collected from July 2017 to July 2020 and analyzed from July 2020 to December 2021.

MAIN OUTCOMES AND MEASURES Two dimensions were identified to delineate LLD-associated heterogeneity in voxelwise GM maps, white matter (WM) fractional anisotropy, neurocognitive functioning, clinical phenotype, and genetics.

RESULTS A total of 501 participants with LLD (mean [SD] age, 67.39 [5.56] years; 332 women) and 495 healthy control individuals (mean [SD] age, 66.53 [5.16] years; 333 women) were included. Patients in dimension 1 demonstrated relatively preserved brain anatomy without WM disruptions relative to healthy control individuals. In contrast, patients in dimension 2 showed widespread brain atrophy and WM integrity disruptions, along with cognitive impairment and higher depression severity. Moreover, 1 de novo independent genetic variant (rs13120336; chromosome: 4, 186387714; minor allele, G) was significantly associated with dimension 1 (odds ratio, 2.35; SE, 0.15; $P = 3.14 \times 10^{8}$) but not with dimension 2. The 2 dimensions demonstrated significant single-nucleotide variant–based heritability of 18% to 27% within the general population (N = 12 518 in UK Biobank). In a subset of individuals having longitudinal measurements, those in dimension 2 experienced a more rapid longitudinal change in GM and brain age (Cohen $f^2 = 0.03$; $P = .02$) and were more likely to progress to Alzheimer disease (Cohen $f^2 = 0.03$; $P = .03$) compared with those in dimension 1 (N = 1431 participants and 7224 scans from the Alzheimer's Disease Neuroimaging Initiative [ADNI], Baltimore Longitudinal Study of Aging [BLSA], and Biomarkers for Older Controls at Risk for Dementia [BIOCARD] data sets).

CONCLUSIONS AND RELEVANCE This study characterized heterogeneity in LLD into 2 dimensions with distinct neuroanatomical, cognitive, clinical, and genetic profiles. This dimensional approach provides a potential mechanism for investigating the heterogeneity of LLD and the relevance of the latent dimensions to possible disease mechanisms, clinical outcomes, and responses to interventions.

JAMA Psychiatry. doi:10.1001/jamapsychiatry.2022.0020
Published online March 9, 2022.

Supplemental content

Author Affiliations: Author affiliations are listed at the end of this article.

Group Information: The members of the ADNI, BIOCARD, BLSA, and iSTAGING study groups appear in Supplements 2, 3, 4, and 5, respectively.

Corresponding Author: Junhao Wen, PhD, Center for Biomedical Image Computing and Analytics, Perelman School of Medicine, University of Pennsylvania, 3700 Hamilton Walk, Philadelphia, PA 19104 (junhao.wen89@gmail.com); Christos Davatzikos, PhD, Center for Biomedical Image Computing and Analytics, Perelman School of Medicine, University of Pennsylvania, 3700 Hamilton Walk, Philadelphia, PA 19104 (christos.davatzikos@pennmedicine.upenn.edu).

Major depressive disorder is one of the most common mental health disorders and is a leading contributor to disability worldwide.[1,2] Late-life depression (LLD) refers to major depressive disorder that is present in individuals 60 to 65 years and older and can be early onset or late onset. LLD affects 1.8% to 7.2% of older adults in the general community.[3,4]

There is considerable heterogeneity in clinical presentation and illness progression in LLD.[5,6] Pharmacological and psychological treatments tend to be less effective in LLD than in other adult age groups. Up to 50% of patients with LLD do not achieve remission with their first treatment.[7] LLD is associated with cognitive impairment[5,6] and high rates of comorbidity, including cardiac and cerebrovascular disease[8] and stroke,[9] as well as increased risk of obesity, diabetes, frailty,[10] and neurodegenerative diseases, such as Alzheimer disease and vascular dementia.[11-14]

Magnetic resonance imaging has revealed gray matter (GM) reductions in bilateral anterior cingulate and medial frontal cortices, insula, putamen, and globus pallidus, extending into the parahippocampal gyrus, amygdala, and hippocampus. In contrast, larger GM volumes have been observed in the lingual gyrus,[15] putamen, and caudate regions.[16] Diffusion tensor imaging demonstrates widespread losses in white matter (WM) integrity, including in the anterior thalamic radiation, cingulum, corticospinal tract, superior and inferior longitudinal fasciculi, and uncinate fasciculus.[17] Collectively, the findings support biological models of LLD being associated with cortical atrophy and WM abnormalities in specific brain networks, although the extent and magnitude vary.

Methodological advancements in data-driven biological subtypes[18-23] are challenging the traditional definition of neurological diseases, such as Alzheimer disease[18,19,21,22] and depressive disorder.[24-26] One of the advantages of semisupervised clustering methods[22,23,27,28] is that they perform subtyping via 1-to-*k* mapping from the domain of a reference group (ie, healthy control individuals) to the patient group, thereby avoiding clustering patients according to disease-irrelevant confounds. Distinct neuropathological mechanisms may underlie heterogeneity in the presentation and progression of the clinical phenotype.[29] Furthermore, the extent to which genetic heterogeneity influences or interacts with phenotypic expression has barely been explored,[30] and individual-level variability, including environment, genetic or other factors, may lead to different levels of disease liability.[31]

We sought to delineate heterogeneity in patients with LLD in a large multicenter sample (N = 996) using a semisupervised clustering method (heterogeneity through discriminative analysis [HYDRA]).[27] We hypothesized that multiple distinct dimensions can describe the underlying heterogeneity and that these dimensions might be prominent in the general population and longitudinal trajectories.

Key Points

Question Is late-life depression (LLD) associated with structural neuroimaging patterns?

Findings In this case-control study, 2 dimensions best represented neuroanatomical heterogeneity in patients with LLD: one was associated with preserved brain structure and the other demonstrated diffuse structural abnormalities and greater cognitive impairment. One de novo independent genetic variant was significantly associated with dimension 1 but not with dimension 2, and dimension 2 was longitudinally associated with Alzheimer disease and brain aging more than dimension 1.

Meaning The 2 dimensions representing heterogeneity in LLD in this study may offer the potential for clinical precision in diagnosis and prognosis.

Methods

Participants

The Imaging-Based Coordinate System for Aging and Neurodegenerative Diseases (iSTAGING) is an international consortium consisting of various imaging protocols, scanners, data modalities, and pathologies,[32] comprising harmonized magnetic resonance imaging data in more than 35 000 participants from more than 13 studies and encompassing a wide range of ages (22 to 90 years). The present study includes patients with LLD from 4 cohorts, including UK Biobank (UKBB),[33,36] Psychotherapy Response Study at the University of California San Francisco (UCSF), Baltimore Longitudinal Study of Aging (BLSA),[34,35] and Biomarkers of Cognitive Decline Among Normal Individuals (BIOCARD). The institutional review board at each site approved the study. All participants provided written informed consent to the studies contributing to this pooled mega-analysis.

We applied a harmonized LLD definition criterion to consolidate participants with LLD and excluded those with comorbid medical and neurological diseases that were potential confounders as follows: all participants from all 4 sites were restricted to be 60 years or older; for UKBB, we excluded individuals who were diagnosed with schizophrenia, bipolar disorder, psychotic symptoms, anxiety, obsessive-compulsive disorder, posttraumatic stress disorder, Huntington disease, Alzheimer disease, epilepsy and stroke, diabetes, or hypertension; for BLSA, we excluded individuals diagnosed with hypertension, anxiety, bipolar disorder, or schizophrenia; for BIOCARD, we excluded individuals diagnosed with diabetes or hypertension; and for UCSF, we excluded individuals with substance misuse, psychotic features, cognitive-enhancing substance use, neurological diseases, or posttraumatic stress disorders (**Table**). We defined 2 additional populations: a general population (12 518 participants from UKBB) and a longitudinal population (1431 participants from ADNI, BLSA, and BIOCARD). A total of 996 participants (501 patients with LLD and 495 healthy control individuals) were included. Image protocols and acquisition parameters for all sites are presented in the eMethods in Supplement 1. The search terms for this study were *late-life depression*, *heterogeneity*, *semisupervised clustering*, and *dimensional representation*. Data were collected from July 2017 to July 2020 and analyzed from July 2020 to December 2021.

Image Preprocessing

Quality-controlled images were corrected for magnetic field intensity inhomogeneity[37] (eMethods in Supplement 1). A mul-

Table. Study Cohort Characteristics

Characteristic	LLD population[a]			General population[b]	Longitudinal population[c]
	Control	LLD	*P* value		
No.	495	501		12 518	1431
Age, median (range), y	66.26 (60.00-91.47)	67.33 (60.00-91.00)	.34	67.23 (60.00-80.00)	71.88 (60.00-93.00)
Sex, No. (%)[d]					
Female	333 (67)	332 (66)	.78	6123 (49)	666 (47)
Male	162 (33)	169 (34)		6395 (51)	765 (53)
Education, mean (SD), y[e]	14.76 (2.68)	14.87 (2.62)	.55	16.90 (2.81)	16.86 (2.57)
Systole, mean (SD), mm Hg[e]	135.03 (16.83)	134.75 (16.56)	.52	140.97 (18.88)	124.06 (2.57)
Diastole, mean (SD), mm Hg[e]	75.59 (9.24)	79.05 (9.15)	.45	82.26 (10.45)	69.93 (11.05)
Age at onset, mean (SD), y[e]	NA	34.62 (15.70)	NA	NA	NA

Abbreviations: LLD, late-life depression; NA, not applicable.

[a] More details on the LLD population are presented in eTable 1 and the eMethods in Supplement 1.

[b] For the general population, we included all individuals from UK Biobank 60 years and older (excluding overlapping individuals in the LLD population). Note that this population is cognitively healthy but might have been diagnosed with other general disorders historically.[36] More details of the general population are presented in eTable 6 in Supplement 1.

[c] For the longitudinal population, we included all healthy control individuals from the Alzheimer's Disease Neuroimaging Initiative, Baltimore Longitudinal Study of Aging, and Biomarkers for Older Controls at Risk for Dementia data sets who were diagnosed as cognitively healthy at baseline. We present here only baseline information. For more details, refer to eTable 7 in Supplement 1.

[d] χ^2 Test of independence was used for categorical variables.

[e] Mann-Whitney *U* (Wilcoxon) test was used for continuous variables.

tiatlas parcellation method (multiatlas region segmentation utilizing ensembles of registration algorithms and parameters, and locally optimal atlas selection [MUSE])[38] was used to extract region-of-interest values of the segmented GM tissue maps (eTable 2 in Supplement 1). Voxelwise regional volumetric maps for each tissue volume[39] were generated by spatially aligning skull-stripped images to a template residing in the Montreal Neurological Institute (MNI) space using a registration method.[40] Fractional anisotropy maps were used to examine microstructural integrity disruptions in the WM (eMethods in Supplement 1). The mean fractional anisotropy values were extracted within the 48 WM tracts of the Johns Hopkins University international consortium for brain mapping diffusion tensor imaging-81 WM label atlas.[41] Intersite image harmonization of the GM MUSE regions of interest is detailed in the eMethods in Supplement 1.

Genetic Preprocessing

We consolidated an imaging-genetic data set from UKBB that passed the quality-control protocol, resulting in 20 438 participants and 8 430 655 single-nucleotide variants (eMethods in Supplement 1). We then selected 774 UKBB participants who overlapped with the LLD population for genetic analyses.

Discovery of the Multidimensional Representation via HYDRA

We applied HYDRA[27] to the harmonized MUSE regions of interest (eMethods in Supplement 1). Briefly, HYDRA aims to cluster disease effects instead of directly clustering participants by comparing the patterns between healthy control individuals and patients with LDD, thus resulting in a 1-to-*k* mapping from the control domain to the patient domain.

We chose the optimal number of dimensions or clusters (*k*), ranging from 2 to 8 clusters, using the adjusted Rand index.[42] We performed additional analyses to evaluate the robustness of the optimal *k* clusters scheme. First, split-sample analyses[43] were carried out to assess whether the dimensions in each half exhibited similar neuroanatomical patterns, given that the 2 halves had similar cohort characteristics in terms of age, sex, and site. Second, we conducted leave-site-out validation[44] to examine whether the dimensions were consistent across sites, training on UKBB only and training on all sites. Lastly, a permutation test was performed to test the statistical significance with the optimal *k* cluster scheme (eMethods in Supplement 1). Statistical significance was set at .05 for a 2-tailed test.

Evaluation of the Multidimensional Representation in Neuroimaging, Cognition, and Genetics

We subsequently investigated the characteristics of the multiple dimensions regarding GM volume, WM integrity, cognitive functioning and depression-related variables, and genetic architecture. Moreover, we investigated the expression of the *k* dimensions in the general population and longitudinal data.

Voxelwise Regional Volumetric GM Maps

Voxelwise regional volumetric GM maps from all sites were used to assess differences in GM tissue volumes. The 3dttest++ program[45] in Analysis of Functional Neuroimages software version 17.2.10 (Medical College of Wisconsin and National Institutes of Health)[46] was used to detect the distinct neuroanatomical patterns of the corresponding dimensions vs the control group, considering age, sex, site, and intracranial volume as covariates. For those voxels that survived the adjustment (Benjamini-Hochberg procedure), voxelwise effect-size maps (ie, Cohen f^2) were estimated for each paired comparison.

Regional WM Integrity Abnormality

WM microstructural abnormality was assessed using the mean fractional anisotropy values of the 48 regional tracts from

UKBB. Group comparisons were performed with multiple linear regression models using R version 3.4.0 (R Foundation) (eMethods in Supplement 1). Age and sex were fixed effects, and group was the variable of interest. *P* values were corrected, and Cohen f^2 was computed with the same procedure as above.

Demographic, Cognitive, and Clinical Variables

Group comparisons for demographic, cognitive, and clinical variables (eTable 5 in Supplement 1) were examined separately between the dimensions. Mann-Whitney *U* (Wilcoxon) test was used for continuous variables (eg, age) and χ^2 test of independence for categorical variables (eg, sex). Global effect size (ie, Cohen *d*) was also reported for continuous variables.

Genome-Wide Associations

We performed genome-wide associations with the derived binary dimension traits (ie, dimension 1 or dimension 2) vs control using PLINK version 2.0 (Massachusetts General Hospital). The Functional Mapping and Annotation (FUMA) online platform version 1.3.6b (Center for Neurogenomics and Cognitive Research)[3] was then used to annotate the genomic risk loci and independent significant single-nucleotide variants (eMethods in Supplement 1).

Evaluation of the Multiple Dimensions in the General Population

The trained model was applied to the external validation samples in the general population (Table). Dimension membership and expression scores of the *k* dimensions were derived (eMethods in Supplement 1).

We examined neuroanatomical patterns using voxelwise regional volumetric GM maps. In addition, demographic and cognitive functioning of the *k* dimensions was investigated in the general population. We calculated the genome-wide single-nucleotide variant-based heritability coefficient (h^2) using Genome-wide Complex Trait Analysis software version 1.93.2β (School of Life Sciences)[4] (eMethods in Supplement 1).

Evaluation of the Multiple Dimensions in Longitudinal Data and Patient Progress to Alzheimer Disease and Brain Aging

The cross-sectionally trained model was applied to the longitudinal population (Table). Dimension membership was derived to evaluate its longitudinal changes in MUSE GM regions of interest using the spatial patterns of atrophy for recognition of Alzheimer disease index[47] and the spatial patterns of atrophy for recognition of brain age index.[48] Specifically, the rate of change over time in these variables for each participant was derived with a linear mixed-effects model and compared across dimensions using a linear regression model (eMethods in Supplement 1).

Results

Two Dimensions Revealed in HYDRA

The highest adjusted Rand index (0.58) was achieved by a HYDRA model for $k = 2$ clusters (eFigure 1 in Supplement 1). The cluster assignment distribution for $k = 2$ to 8 across sites is presented in eTable 3 in Supplement 1. For the optimal $k = 2$ clustering scheme, 227 participants with LLD were assigned to dimension 1 and 274 to dimension 2. The optimal $k = 2$ clustering scheme was replicated in split-sample and leave-site-out analyses (eFigure 1 in Supplement 1). In the leave-site-out analyses, the percentage overlap for participants assigned to the same dimension was 446 of 501 (89.02%) (369 of 402 [92%] for UKBB, 22 of 29 [76%] for BLSA, 4 of 5 [80%] for BIOCARD, and 51 of 65 [78%] for UCSF). The neuroanatomical patterns of the 2 dimensions were similar (eFigure 3 in Supplement 1) to the original dimension patterns (**Figure 1**). In split-sample analyses, the GM patterns for the 2 splits were similar (eFigure 2 in Supplement 1) compared with the original dimension patterns (Figure 1). The adjusted Rand index at $k = 2$ was higher than the null distribution in the permutation test (Cohen *d*, 0.31; 95% CI, 0.13-0.49; $P < .001$). Lastly, we presented the results without excluding comorbidities in UKBB, which yielded similar imaging patterns for the 2 dimensions (eFigure 4 in Supplement 1). Therefore, we present the results of $k = 2$ for all subsequent analyses.

Differences in GM Volumetric Patterns

Patients in dimension 1 demonstrated greater GM tissue volume in bilateral thalamus, putamen, and caudate relative to healthy control individuals. Those in dimension 2 demonstrated reduced GM tissue volume in widespread cortical regions, including bilateral anterior and posterior cingulate gyri, superior, middle, and inferior frontal gyri, gyrus recti, insular cortices, superior, middle, and inferior temporal gyri compared with control individuals (Figure 1). The split-sample and leave-site-out analyses in support are detailed in eFigures 2 and 3 in Supplement 1, respectively.

Differences in WM Integrity Disruption

Patients in dimension 1 exhibited similar fractional anisotropy values compared with control individuals. However, those in dimension 2 showed widespread WM disruptions, with 31 of the 48 WM tracts demonstrating significantly lower fractional anisotropy values than in control individuals but small effect sizes ($0.01 \leq$ Cohen $f^2 \leq 0.05$, Figure 1B). Specifically, the middle cerebellar peduncle tract obtained the highest effect size (Cohen $f^2 = 0.05$). Other affected WM tracts mainly involved the frontal lobe and subcortical limbic regions (eTable 4 in Supplement 1).

Differences in Clinical Profiles by Dimension

Patients in dimension 1 showed statistically higher scores in fluid intelligence scores (Cohen *d*, 0.25; 95% CI, 0.09-0.41), fewer errors in pairs matching test (Cohen *d*, −0.28; 95% CI, −0.41 to −0.15), and fewer depressive symptoms in patient health questionnaire responses (Cohen *d*, −0.45; 95% CI, −0.95 to 0.05) relative to dimension 2. The 2 dimensions did not significantly differ in age, sex, site, or other clinical variables (details in eTable 5 in Supplement 1).

Differences in Genome-Wide Associations

Dimension 1, but not dimension 2, was significantly associated with 1 de novo independent variant (rs13120336; chro-

Figure 1. Distinct Structural Patterns in Dimensions 1 and 2

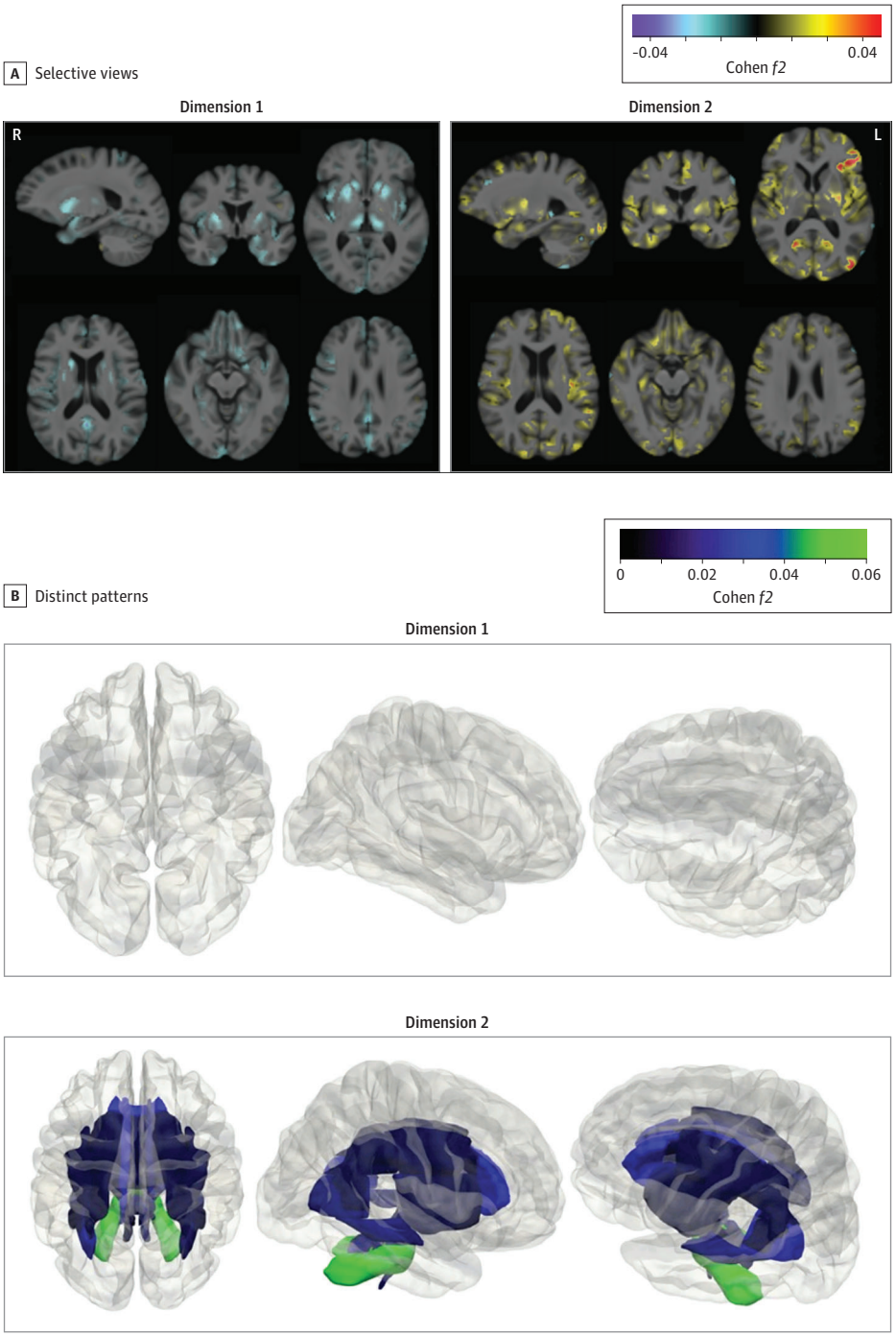

Effect size maps were identified in dimension 1 and dimension 2 compared with control individuals, respectively. A, Warmer color denotes brain atrophy (ie, control > dimension), and cooler color represents larger tissue volume (ie, dimension > control). Both directions are shown for each dimension. L indicates left; R, right. The effect size map is shown in a radiological fashion such that the left of the brain is shown to the right of the display. B, Dimensions 1 and 2 demonstrated 2 distinct white matter (WM) patterns based on fractional anisotropy values. Patients in dimension 1 exhibited a normal appearance without significant difference from control individuals, whereas those in dimension 2 showed widespread disruptions in WM integrity. The *P* value and effect size for all 48 WM tracts are shown in eTable 4 in Supplement 1. Both directions of the comparisons were performed, but effect sizes only show WM integrity disruptions. For reference, Cohen f^2 values of ≥0.02, ≥0.15, and ≥0.35 signify small, moderate, and large effect sizes, respectively. We do not claim that voxel-based differences provide validation of clustering. We simply show these comparisons to elucidate the characteristics of the dimensions determined by the machine learning algorithm so that we can appreciate the features that were found by the algorithm to be essential for the definition of these dimensions.

mosome: 4, 186387714; minor allele, G)[5] (odds ratio, 2.35; SE, 0.15; $P = 3.14 \times 10^{8}$) (**Figure 2**). Quantile-quantile plots are presented in eFigure 5 in Supplement 1.

Expression of the 2 Dimensions in the General Population

Applying the trained model to UKBB samples resulted in 2269 participants in dimension 1, 3786 in dimension 2, 2963 in whom both dimensions were expressed, and 3500 in whom neither dimension was expressed (eTable 6 in Supplement 1; **Figure 3**).

The neuroanatomical patterns of the 2 dimensions were stable (Figure 3). Participants in dimension 1 showed higher scores in fluid intelligence scores (Cohen *d*, 0.28; 95% CI, 0.22-0.34; $P < .001$), but lower errors in pairs matching (Cohen *d*, −0.13; 95% CI, −0.18 to −0.08; $P < .001$) compared with those in dimension 2 (eTable 6 in Supplement 1). The expression scores of the 2 dimensions were significantly heritable in the general population. Specifically, h^2 was 0.27 (SE, 0.04; $P < .001$) for dimension 1 and 0.18 (SE, 0.04; $P < .001$) for dimension 2.

Figure 2. Distinct Genetic Profiles in the Genome-Wide Association Study (GWAS) Between Dimensions 1 and 2

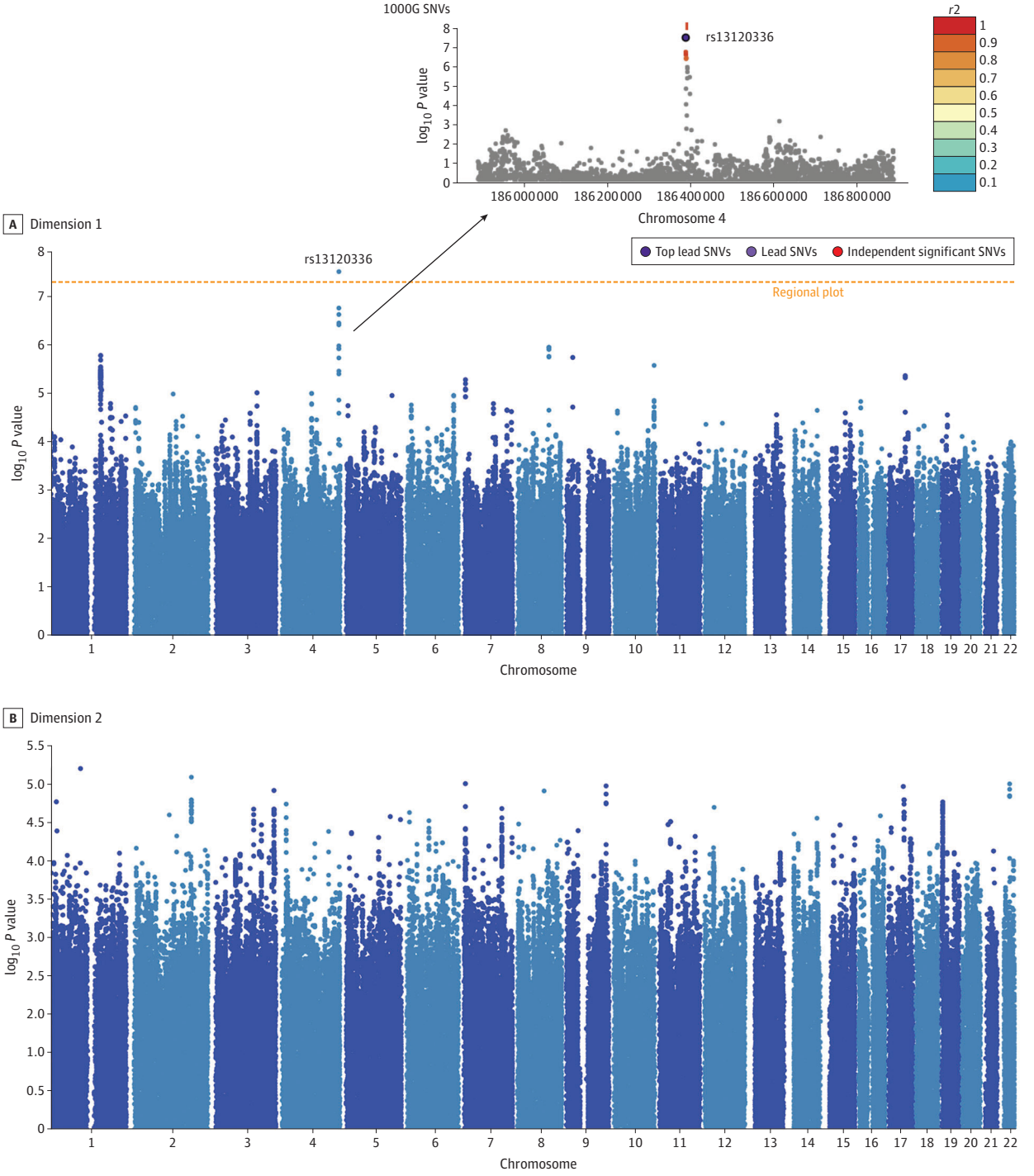

A, Dimension 1 was significantly associated with a novel genomic risk locus. This significant independent single-nucleotide variant (SNV) (rs13120336) is in linkage disequilibrium with other 7-candidate SNVs that passed the GWAS *P* value threshold (5e-8). Functional Mapping and Annotation identified 2 corresponding protein-encoding genes: *CCDC110* and *LOC105377590*. B, Dimension 2 was not significantly associated with any variants.

The 2 Dimensions and Longitudinal Trajectories

Applying the trained model to ADNI, BLSA, and BIOCARD, which also had longitudinal follow-up data, yielded 301 participants in dimension 1, 390 in dimension 2, 330 in whom both dimensions were expressed, and 410 in whom neither dimension was expressed in baseline images (eTable 7 in Supplement 1). The neuroanatomical patterns of the 2 dimensions were stable (eFigure 6 in Supplement 1). The GM

Figure 3. Expression of the 2 Dimensions in the General Population

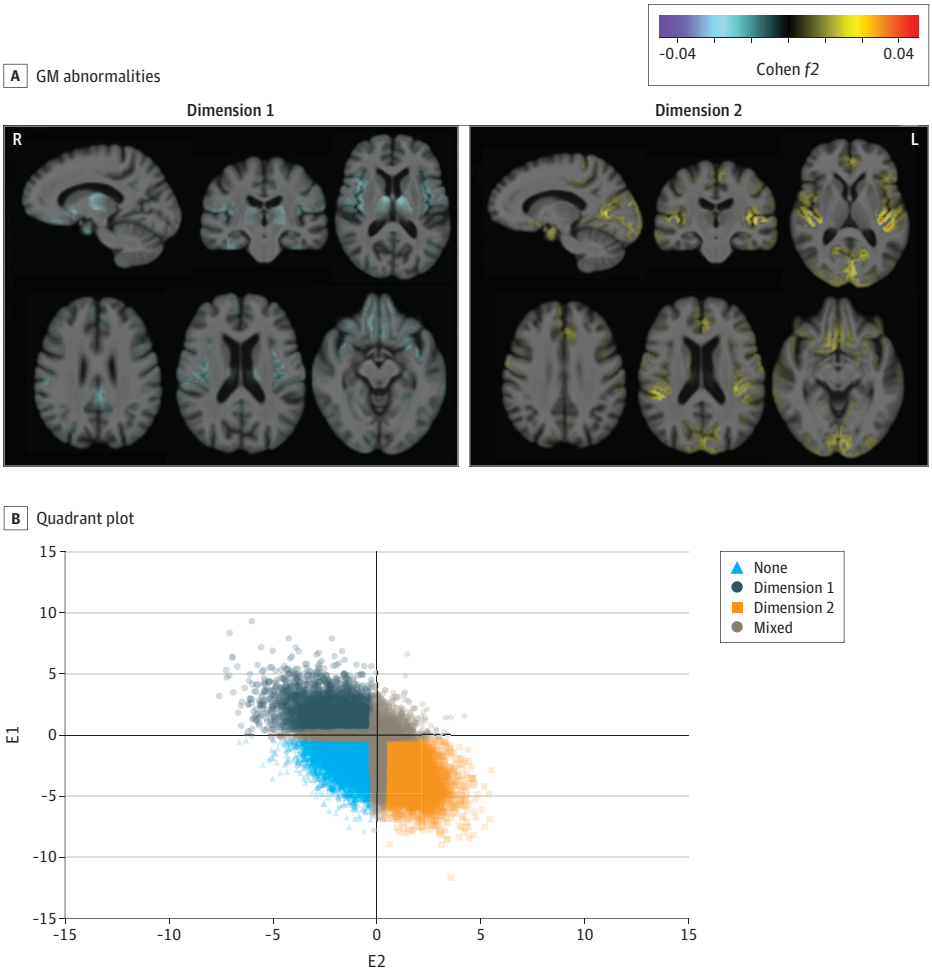

A, The 2 neuroanatomical dimensions in UK Biobank (UKBB) show distinct gray matter (GM) abnormalities. Effect size maps of GM patterns were identified in dimension 1 and dimension 2 compared with none (the dimension that does not express in dimension 1 or 2), respectively. Multiple selective views are shown with the number of slices in the axial view. Warmer color denotes brain atrophy (ie, none > dimension), and cooler color represents larger tissue volume (ie, dimension > none). Both directions are shown for each dimension. Cohen f^2 of ≥0.02, ≥0.15, and ≥0.35 signify small, moderate, and large effect sizes, respectively. L indicates left; R, right. The effect size map is shown in a radiological fashion such that the left of the brain is shown to the right of the display. We include age, sex, and intracranial volume as fixed effects and group (none vs dimension 1 or dimension 2) as the variable of interest. The likelihood ratio test was used to test each effect. B, The quadrant plot after applying the heterogeneity through discriminative analysis model trained on the late-life depression population to the external UKBB individuals. The x-axis and y-axis represent the expression scores for each individual at dimension 1 and dimension 2, respectively. Dimension membership was decided based on the 2 expression scores, E1 and E2. Specifically, an individual was assigned to none when E1 and E2 were less than −0.3, as dimension 1 when E1 was less than 0.3 and E2 less than −0.3, as dimension 2 when E1 was less than−0.3 and E2 greater than 0.3, and as mixed for the other individuals.

rate of change in participants in dimension 2 decreased more rapidly than it did in those in dimension 1 or neither dimension (−0.1 < Cohen f^2 < 0.1), specifically in the left precentral gyrus, temporal pole, and right anterior insula (eFigure 6 in Supplement 1). Moreover, the 2 dimensions remained independent and stable along longitudinal trajectories (**Figure 4**). Patients in dimension 2 showed progression of both spatial patterns of atrophy for recognition of Alzheimer disease (Cohen f^2 = 0.03) and spatial patterns of atrophy for recognition of brain atrophy (Cohen f^2 = 0.03) compared with those in dimension 1 (Figure 4B), but not at baseline.

Discussion

Two reproducible and distinct dimensions characterized neuroanatomical heterogeneity in patients with LLD. Patients in dimension 1 showed relatively preserved brain anatomy with larger subcortical regional volumes and were more likely to have with 1 de novo genetic variant, while those in dimension 2 displayed widespread brain atrophy and WM integrity disruptions with impaired cognitive functioning and increased depressive severity. Moreover, the 2 dimensions were

Figure 4. The 2 Dimensions and Longitudinal Trajectories to Aging and Alzheimer Disease

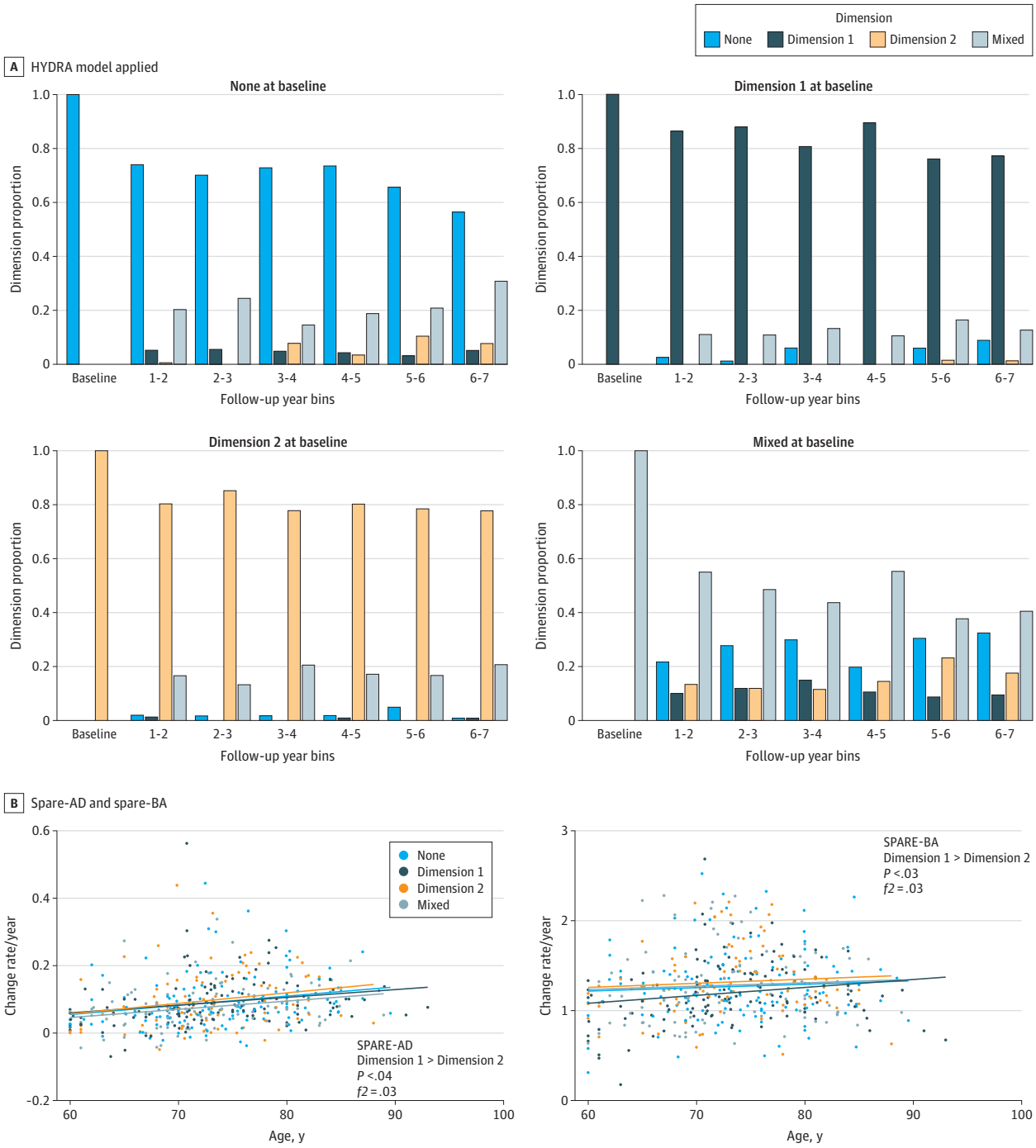

A, Applying the heterogeneity through discriminative analysis (HYDRA) model to all available longitudinal scans with at least 6 years of follow-up. The 2 dimensions remained stable over time and were independent of each other. B, The positive rate of change for spatial patterns of atrophy for recognition of Alzheimer disease (SPARE-AD), and the spatial patterns of atrophy for recognition of brain atrophy (SPARE-BA) of dimension 2 was bigger than dimension 1, meaning that patients in dimension 2 were more vulnerable to Alzheimer disease and brain aging longitudinally. Only individuals that had at least 6 time points were included for this analysis.

manifested in the general population and were significantly heritable. Notably, patients in dimension 2 demonstrated a higher degree of progression to AD and brain aging signatures relative to dimension 1.

The 2 dimensions demonstrated the extent of underlying GM heterogeneity in patients with LLD. GM atrophy evident in dimension 2 has been widely reported in previous case-control studies.[49-51] Regional atrophy in the frontal lobes has

been observed,[52,53] which is associated with cognitive deficits as well as reports of psychotic symptoms.[54] Striatal atrophy has been associated with degeneration in the dopaminergic connections between caudate and cortical limbic areas involved in mood regulation,[55] although increased caudate and putamen volumes have been found in UKBB depression phenotypes.[16] Dimension 2 showed atrophy in hippocampal regions, perhaps indicative of future neuroprogressive degeneration associated with Alzheimer disease.

The 2 identified neuroanatomical dimensions differed significantly in microstructural integrity. Dimension 1 showed no significant WM abnormalities, while dimension 2 demonstrated widespread WM abnormalities. WM lesions may play a key role in conferring vulnerability or perpetuating depressive syndromes in patients with LLD and contributing to the observed microstructural disturbance.[56] Widespread WM disruptions can persist in patients with LLD, even excluding WM lesions from the diffusion tensor imaging analysis.[57] WM tracts connecting frontosubcortical and frontolimbic regions are most frequently affected, including the uncinate fasciculus,[58,59] anterior thalamic radiation, superior longitudinal fasciculus,[56,58,60] and posterior cingulate cortex.[61] Dimension 2 demonstrated clinical features of patients with LLD that are frequently associated with more severe cognitive deterioration.[62-64] Interestingly, previous studies using depressive symptom and cognitive scores,[25] or metabolic-inflammatory profile,[26] derived 1 subtype that was a healthy group and other subgroups that demonstrated higher depressive symptom scores or a more specific immune-inflammatory dysregulation profile.

The detected genetic variant (rs13120336) was uniquely associated with dimension 1. Two mapped genes (*CCDC110* and *LOC105377590*) have been previously associated with cancer and diabetes.[65,66] We speculate that these genetic factors may play a key role in the heterogeneity of imaging phenotype and cognitive dysfunctions in the 2 dimensions. Many studies have shown that depression is associated with different genetic variants, some of which were not replicated.[67-70] Replication needs to be performed to confirm this detected variant. In general, our dimensional approach might provide another approach for genetic associations in depression.

The 2 dimensions showed significant genetic heritability of 18% to 27%, potentially suggesting genetic underpinnings of neuroanatomical phenotypes associated with depression in the general population. Multimorbidity, such as schizophrenia and anxiety disorders, in the UKBB population[71] might partially account for the expression of the 2 dimensions. Major depressive disorder is a common and complex syndrome with an estimated genetic heritability of approximately 40%,[72] and prevalence rates range from 7% to 13%.[70] Our findings confirm the high risks and prevalence of depression in the general population.

The 2-dimensional representation proposed in this study emphasizes the prognostic potential to distinguish LLD that cooccurs with or precedes neurodegenerative diseases. Patients in dimension 2 progressed toward Alzheimer disease or brain aging, whereas those in dimension 1 expressed a preserved brain anatomy. Epidemiological studies[73,74] have consistently found that shared risk factors exist in Alzheimer disease and LLD, supporting depression as a prodromal feature or a risk factor associated with Alzheimer disease. The 2 dimensions did not longitudinally differ in cognitive impairment, perhaps supporting the Alzheimer disease pathological cascade model.[75]

To ensure the reproducibility of the findings, we performed split-sample analysis, leave-site-out analysis, and applying the model trained on LLD to independent UKBB and a combined ADNI, BLSA, and BIOCARD cohort with the same age range as the LLD population. From a technical perspective, applying the trained LLD model to a younger population would be possible, but this could lead to a trivial solution owing to the significant difference in age ranges rather than a disease effect of interest, as aging might play a crucial role in driving these dimensions. We believe that applying the model to external data requires careful consideration of potential confounds, such as demographic differences.

Limitations

This study has limitations. First, longitudinal data in LLD are needed to confirm the added value of the proposed multidimensional representation. Additionally, replication of the genome-wide association findings is required when additional data are available.

Conclusions

In this study, LLD was characterized into 2 dimensions associated with neuroanatomy, cognitive functioning, and genetic profiles. The 2-dimensional representation offers a potential system for future research on the underlying etiology mechanisms and heterogeneity of genetic architectures as well as personalized clinical care.

ARTICLE INFORMATION

Accepted for Publication: December 19, 2021.

Published Online: March 9, 2022. doi:10.1001/jamapsychiatry.2022.0020

Author Affiliations: Center for Biomedical Image Computing and Analytics, Perelman School of Medicine, University of Pennsylvania, Philadelphia (Wen, Yang, Abdulkadir, Mamourian, Srinivasan, Skampardoni, Singh, Nawani, Erus, Shou, Doshi, Fan, Wolk, Davatzikos); University of East London, School of Psychology, London, United Kingdom (Fu); Centre for Affective Disorders, Institute of Psychiatry, Psychology and Neuroscience, King's College London, London, United Kingdom (Fu); Department of Radiology and Biomedical Imaging, University of California, San Francisco (Tosun); Department of Genetics and Institute for Biomedical Informatics, Perelman School of Medicine, University of Pennsylvania, Philadelphia (Veturi, Ritchie); Department of Biostatistics, Epidemiology and Informatics, Perelman School of Medicine, University of Pennsylvania, Philadelphia (Bao, Shen); Penn Statistics in Imaging and Visualization Center, Department of Biostatistics, Epidemiology, and Informatics, Perelman School of Medicine, University of Pennsylvania, Philadelphia (Shou); Glenn Biggs Institute for Alzheimer's & Neurodegenerative Diseases, University of Texas Health Science Center at San Antonio, San Antonio (Habes); Department of Statistics, Center for Theoretical Neuroscience, Zuckerman Institute, Columbia University, New York, New York (Varol); Department of Psychiatry and Behavioral Sciences, University of California, San Francisco (Mackin); Department of Radiology and Institute for Informatics, Washington University School of Medicine, St Louis, Missouri (Sotiras); Radiology and Imaging Sciences, Center for Neuroimaging,

Department of Radiology and Imaging Sciences, Indiana Alzheimer's Disease Research Center and the Melvin and Bren Simon Cancer Center, Indiana University School of Medicine, Indianapolis (Saykin); Center for Neuromodulation in Depression and Stress, Department of Psychiatry, Perelman School of Medicine, University of Pennsylvania, Philadelphia (Sheline); Department of Neurology and Penn Memory Center, University of Pennsylvania, Philadelphia (Wolk); Department of Neurology, Johns Hopkins University School of Medicine, Baltimore, Maryland (Albert); Laboratory of Behavioral Neuroscience, National Institute on Aging, Baltimore, Maryland (Resnick).

Author Contributions: Dr Wen and Dr Davatzikos had full access to all the data in the study and take responsibility for the integrity of the data and the accuracy of the data analysis.
Study concept and design: Davatzikos, Wen, Fu
Acquisition, analysis, or interpretation of data: Davatzikos, Wen, Fu, Tosun, Resnick
Drafting of the manuscript: Wen, Fu
Critical revision of the manuscript for important intellectual content: Wen, Fu, Tosun, Veturi, Yang, Mamourian, Srinivasan, Skampardoni, Singh, Nawani, Bao, Erus, Shou, Abdulkadir, Habes, Doshi, Varol, Mackin, Sotiras, Fan, Sheline, Saykin, Shen, Ritchie, Wolk, Albert, Resnick, Davatzikos
Statistical and genetic analysis: Wen
Obtained funding: Davatzikos
Administrative, technical, or material support: Davatzikos
Supervision: Davatzikos, Fu

Conflict of Interest Disclosures: Dr Mackin reported grants from the National Institutes of Health during the conduct of the study and outside the submitted work and support from Johnson and Johnson outside the submitted work. Dr Sotiras reported support from TheraPanacea Equity outside the submitted work. Dr Saykin reported grants from the National Institutes of Health paid to Indiana University during the conduct of the study. Dr Saykin receives support from multiple National Institutes of Health grants, has received support from Avid Radiopharmaceuticals, a subsidiary of Eli Lilly (in kind contribution of PET tracer precursor); Bayer Oncology (scientific advisory board); Siemens Medical Solutions (dementia advisory board); Springer-Nature Publishing (editorial office support as Editor-in-Chief, Brain Imaging and Behavior). Dr Wolk served as site principle investigator for studies by Biogen, Merck, and Eli Lilly/Avid; has received consulting fees from General Electric Healthcare and Neuronix; is on the DSMB for a trial sponsored by Functional Neuromodulation; and has consulted for Qynapse. Dr Albert reported grants from the National Institute on Aging during the conduct of the study and other support from Eli Lilly Consultant outside the submitted work. No other disclosures were reported.

Funding/Support: This work was supported in part by National Institutes of Health grants 1RF1-AG054409-01 and U01-AG068057. Alzheimer's Disease Neuroimaging Initiative (ADNI) is supported by National Institutes of Health grants U01-AG024904 and RC2-AG036535. The Biomarkers for Older Controls at Risk for Dementia (BIOCARD) study is supported by National Institutes of Health grant U19-AG033655. The Baltimore Longitudinal Study of Aging (BLSA) is supported by the Intramural Research Program of the National Institute on Aging and research and development contract HHSN-260-2004-00012C. This research has been conducted using the UK Biobank Resource under application number 35148.

Role of the Funder/Sponsor: The funders had no role in the design and conduct of the study; collection, management, analysis, and interpretation of the data; preparation, review, or approval of the manuscript; and decision to submit the manuscript for publication.

Group Information: The members of ADNI can be found in Supplement 2, members of BIOCARD in Supplement 3, members of BLSA in Supplement 4, and members of the iSTAGING consortium in Supplement 5.

REFERENCES

1. Belmaker RH, Agam G. Major depressive disorder. *N Engl J Med*. 2008;358(1):55-68. doi:10.1056/NEJMra073096

2. Thornicroft G, Chatterji S, Evans-Lacko S, et al. Undertreatment of people with major depressive disorder in 21 countries. *Br J Psychiatry*. 2017;210(2):119-124. doi:10.1192/bjp.bp.116.188078

3. Beekman AT, Copeland JR, Prince MJ. Review of community prevalence of depression in later life. *Br J Psychiatry*. 1999;174:307-311. doi:10.1192/bjp.174.4.307

4. Luppa M, Sikorski C, Luck T, et al. Age- and gender-specific prevalence of depression in latest-life—systematic review and meta-analysis. *J Affect Disord*. 2012;136(3):212-221. doi:10.1016/j.jad.2010.11.033

5. Alexopoulos GS. Mechanisms and treatment of late-life depression. *Transl Psychiatry*. 2019;9(1):188. doi:10.1038/s41398-019-0514-6

6. Brodaty H, Luscombe G, Peisah C, Anstey K, Andrews G. A 25-year longitudinal, comparison study of the outcome of depression. *Psychol Med*. 2001;31(8):1347-1359. doi:10.1017/S0033291701004743

7. Gutsmiedl K, Krause M, Bighelli I, Schneider-Thoma J, Leucht S. How well do elderly patients with major depressive disorder respond to antidepressants: a systematic review and single-group meta-analysis. *BMC Psychiatry*. 2020;20(1):102. doi:10.1186/s12888-020-02514-2

8. Daskalopoulou M, George J, Walters K, et al. Depression as a risk factor for the initial presentation of twelve cardiac, cerebrovascular, and peripheral arterial diseases: data linkage study of 1.9 million women and men. *PLoS One*. 2016;11(4):e0153838. doi:10.1371/journal.pone.0153838

9. Pan A, Sun Q, Okereke OI, Rexrode KM, Hu FB. Depression and risk of stroke morbidity and mortality: a meta-analysis and systematic review. *JAMA*. 2011;306(11):1241-1249. doi:10.1001/jama.2011.1282

10. Buigues C, Padilla-Sánchez C, Garrido JF, Navarro-Martínez R, Ruiz-Ros V, Cauli O. The relationship between depression and frailty syndrome: a systematic review. *Aging Ment Health*. 2015;19(9):762-772. doi:10.1080/13607863.2014.967174

11. Adler G, Chwalek K, Jajcevic A. Six-month course of mild cognitive impairment and affective symptoms in late-life depression. *Eur Psychiatry*. 2004;19(8):502-505. doi:10.1016/j.eurpsy.2004.09.003

12. Diniz BS, Butters MA, Albert SM, Dew MA, Reynolds CF III. Late-life depression and risk of vascular dementia and Alzheimer's disease: systematic review and meta-analysis of community-based cohort studies. *Br J Psychiatry*. 2013;202(5):329-335. doi:10.1192/bjp.bp.112.118307

13. Galts CPC, Bettio LEB, Jewett DC, et al. Depression in neurodegenerative diseases: Common mechanisms and current treatment options. *Neurosci Biobehav Rev*. 2019;102:56-84. doi:10.1016/j.neubiorev.2019.04.002

14. Reynolds CF, Lenze E, Mulsant BH. Assessment and treatment of major depression in older adults. In: Dekosky ST, Asthana S, eds. *Handbook of Clinical Neurology*. Elsevier; 2019:429-435.

15. Du M, Liu J, Chen Z, et al. Brain grey matter volume alterations in late-life depression. *J Psychiatry Neurosci*. 2014;39(6):397-406. doi:10.1503/jpn.130275

16. Harris MA, Cox SR, de Nooij L, et al. The influence of phenotyping method on structural neuroimaging associations with depression in UK Biobank. *medRxiv*. Preprint posted online December 20, 2020. doi:10.1101/2020.12.18.20248488

17. Wen M-C, Steffens DC, Chen M-K, Zainal NH. Diffusion tensor imaging studies in late-life depression: systematic review and meta-analysis. *Int J Geriatr Psychiatry*. 2014;29(12):1173-1184. doi:10.1002/gps.4129

18. Young AL, Marinescu RV, Oxtoby NP, et al; Genetic FTD Initiative (GENFI); Alzheimer's Disease Neuroimaging Initiative (ADNI). Uncovering the heterogeneity and temporal complexity of neurodegenerative diseases with Subtype and Stage Inference. *Nat Commun*. 2018;9(1):4273. doi:10.1038/s41467-018-05892-0

19. Zhang X, Mormino EC, Sun N, Sperling RA, Sabuncu MR, Yeo BT; Alzheimer's Disease Neuroimaging Initiative. Bayesian model reveals latent atrophy factors with dissociable cognitive trajectories in Alzheimer's disease. *Proc Natl Acad Sci U S A*. 2016;113(42):E6535-E6544. doi:10.1073/pnas.1611073113

20. Eshaghi A, Young AL, Wijeratne PA, et al. Identifying multiple sclerosis subtypes using unsupervised machine learning and MRI data. *Nat Commun*. 2021;12(1):2078. doi:10.1038/s41467-021-22265-2

21. Vogel JW, Young AL, Oxtoby NP, et al; Alzheimer's Disease Neuroimaging Initiative. Four distinct trajectories of tau deposition identified in Alzheimer's disease. *Nat Med*. 2021;27(5):871-881. doi:10.1038/s41591-021-01309-6

22. Yang Z, Nasrallah IM, Shou H, et al; iSTAGING Consortium; Baltimore Longitudinal Study of Aging (BLSA); Alzheimer's Disease Neuroimaging Initiative (ADNI). A deep learning framework identifies dimensional representations of Alzheimer's Disease from brain structure. *Nat Commun*. 2021;12(1):7065. doi:10.1038/s41467-021-26703-z

23. Wen J, Varol E, Sotiras A, et al; Alzheimer's Disease Neuroimaging Initiative. Multi-scale semi-supervised clustering of brain images: Deriving disease subtypes. *Med Image Anal*. 2022;75:102304. doi:10.1016/j.media.2021.102304

24. Drysdale AT, Grosenick L, Downar J, et al. Resting-state connectivity biomarkers define neurophysiological subtypes of depression. *Nat Med*. 2017;23(1):28-38. doi:10.1038/nm.4246

25. Lugtenburg A, Zuidersma M, Wardenaar KJ, et al. Subtypes of late-life depression: a data-driven approach on cognitive domains and physical frailty. *J Gerontol A Biol Sci Med Sci*. 2021;76(1):141-150. doi:10.1093/gerona/glaa110

26. Kokkeler KJE, Marijnissen RM, Wardenaar KJ, et al. Subtyping late-life depression according to inflammatory and metabolic dysregulation: a prospective study. *Psychol Med*. 2020;1-11. doi:10.1017/S0033291720002159

27. Varol E, Sotiras A, Davatzikos C; Alzheimer's Disease Neuroimaging Initiative. HYDRA: Revealing heterogeneity of imaging and genetic patterns through a multiple max-margin discriminative analysis framework. *Neuroimage*. 2017;145(Pt B):346-364. doi:10.1016/j.neuroimage.2016.02.041

28. Dong A, Honnorat N, Gaonkar B, Davatzikos C. CHIMERA: clustering of heterogeneous disease effects via distribution matching of imaging patterns. *IEEE Trans Med Imaging*. 2016;35(2):612-621. doi:10.1109/TMI.2015.2487423

29. Fu CHY, Fan Y, Davatzikos C. Addressing heterogeneity (and homogeneity) in treatment mechanisms in depression and the potential to develop diagnostic and predictive biomarkers. *Neuroimage Clin*. 2019;24:101997. doi:10.1016/j.nicl.2019.101997

30. Tsang RSM, Mather KA, Sachdev PS, Reppermund S. Systematic review and meta-analysis of genetic studies of late-life depression. *Neurosci Biobehav Rev*. 2017;75:129-139. doi:10.1016/j.neubiorev.2017.01.028

31. Cai N, Choi KW, Fried EI. Reviewing the genetics of heterogeneity in depression: operationalizations, manifestations and etiologies. *Hum Mol Genet*. 2020;29(R1):R10-R18. doi:10.1093/hmg/ddaa115

32. Habes M, Pomponio R, Shou H, et al; iSTAGING consortium, the Preclinical AD consortium, the ADNI, and the CARDIA studies. The Brain Chart of Aging: Machine-learning analytics reveals links between brain aging, white matter disease, amyloid burden, and cognition in the iSTAGING consortium of 10,216 harmonized MR scans. *Alzheimers Dement*. 2021;17(1):89-102. doi:10.1002/alz.12178

33. Miller KL, Alfaro-Almagro F, Bangerter NK, et al. Multimodal population brain imaging in the UK Biobank prospective epidemiological study. *Nat Neurosci*. 2016;19(11):1523-1536. doi:10.1038/nn.4393

34. Resnick SM, Pham DL, Kraut MA, Zonderman AB, Davatzikos C. Longitudinal magnetic resonance imaging studies of older adults: a shrinking brain. *J Neurosci*. 2003;23(8):3295-3301. doi:10.1523/JNEUROSCI.23-08-03295.2003

35. Resnick SM, Goldszal AF, Davatzikos C, et al. One-year age changes in MRI brain volumes in older adults. *Cereb Cortex*. 2000;10(5):464-472. doi:10.1093/cercor/10.5.464

36. UKBIOBANK. Data-Field 41202: diagnoses—main *ICD10*. Accessed December 23, 2021. https://biobank.ctsu.ox.ac.uk/crystal/field.cgi?id=41202

37. Tustison NJ, Avants BB, Cook PA, et al. N4ITK: improved N3 bias correction. *IEEE Trans Med Imaging*. 2010;29(6):1310-1320. doi:10.1109/TMI.2010.2046908

38. Doshi J, Erus G, Ou Y, et al; Alzheimer's Neuroimaging Initiative. MUSE: MUlti-atlas region Segmentation utilizing Ensembles of registration algorithms and parameters, and locally optimal atlas selection. *Neuroimage*. 2016;127:186-195. doi:10.1016/j.neuroimage.2015.11.073

39. Davatzikos C, Genc A, Xu D, Resnick SM. Voxel-based morphometry using the RAVENS maps: methods and validation using simulated longitudinal atrophy. *Neuroimage*. 2001;14(6):1361-1369. doi:10.1006/nimg.2001.0937

40. Ou Y, Sotiras A, Paragios N, Davatzikos C. DRAMMS: Deformable registration via attribute matching and mutual-saliency weighting. *Med Image Anal*. 2011;15(4):622-639. doi:10.1016/j.media.2010.07.002

41. Hua K, Zhang J, Wakana S, et al. Tract probability maps in stereotaxic spaces: analyses of white matter anatomy and tract-specific quantification. *Neuroimage*. 2008;39(1):336-347. doi:10.1016/j.neuroimage.2007.07.053

42. Hubert L, Arabie P. Comparing partitions. *J Classif*. 1985;2:193-218. doi:10.1007/BF01908075

43. Ben-Hur A, Elisseeff A, Guyon I. A stability based method for discovering structure in clustered data. *Pac Symp Biocomput*. 2002;6-17.

44. Arlot S, Celisse A. A survey of cross-validation procedures for model selection. *Stat Surv*. 2010;4:40-79. doi:10.1214/09-SS054

45. Cox RW, Chen G, Glen DR, Reynolds RC, Taylor PA. fMRI clustering and false-positive rates. *Proc Natl Acad Sci U S A*. 2017;114(17):E3370-E3371. doi:10.1073/pnas.1614961114

46. Cox RW. AFNI: software for analysis and visualization of functional magnetic resonance neuroimages. *Comput Biomed Res*. 1996;29(3):162-173. doi:10.1006/cbmr.1996.0014

47. Davatzikos C, Xu F, An Y, Fan Y, Resnick SM. Longitudinal progression of Alzheimer's-like patterns of atrophy in normal older adults: the SPARE-AD index. *Brain*. 2009;132(Pt 8):2026-2035. doi:10.1093/brain/awp091

48. Habes M, Erus G, Toledo JB, et al. White matter hyperintensities and imaging patterns of brain ageing in the general population. *Brain*. 2016;139(Pt 4):1164-1179. doi:10.1093/brain/aww008

49. Andreescu C, Butters MA, Begley A, et al. Gray matter changes in late life depression--a structural MRI analysis. *Neuropsychopharmacology*. 2008;33(11):2566-2572. doi:10.1038/sj.npp.1301655

50. Ballmaier M, Narr KL, Toga AW, et al. Hippocampal morphology and distinguishing late-onset from early-onset elderly depression. *Am J Psychiatry*. 2008;165(2):229-237. doi:10.1176/appi.ajp.2007.07030506

51. Bell-McGinty S, Butters MA, Meltzer CC, Greer PJ, Reynolds CF III, Becker JT. Brain morphometric abnormalities in geriatric depression: long-term neurobiological effects of illness duration. *Am J Psychiatry*. 2002;159(8):1424-1427. doi:10.1176/appi.ajp.159.8.1424

52. Lavretsky H, Ballmaier M, Pham D, Toga A, Kumar A. Neuroanatomical characteristics of geriatric apathy and depression: a magnetic resonance imaging study. *Am J Geriatr Psychiatry*. 2007;15(5):386-394. doi:10.1097/JGP.0b013e3180325a16

53. Lavretsky H, Roybal DJ, Ballmaier M, Toga AW, Kumar A. Antidepressant exposure may protect against decrement in frontal gray matter volumes in geriatric depression. *J Clin Psychiatry*. 2005;66(8):964-967. doi:10.4088/JCP.v66n0801

54. Elderkin-Thompson V, Hellemann G, Pham D, Kumar A. Prefrontal brain morphology and executive function in healthy and depressed elderly. *Int J Geriatr Psychiatry*. 2009;24(5):459-468. doi:10.1002/gps.2137

55. Krishnan KR, McDonald WM, Escalona PR, et al. Magnetic resonance imaging of the caudate nuclei in depression. preliminary observations. *Arch Gen Psychiatry*. 1992;49(7):553-557. doi:10.1001/archpsyc.1992.01820070047007

56. Dalby RB, Frandsen J, Chakravarty MM, et al. Depression severity is correlated to the integrity of white matter fiber tracts in late-onset major depression. *Psychiatry Res*. 2010;184(1):38-48. doi:10.1016/j.pscychresns.2010.06.008

57. Shimony JS, Sheline YI, D'Angelo G, et al. Diffuse microstructural abnormalities of normal-appearing white matter in late life depression: a diffusion tensor imaging study. *Biol Psychiatry*. 2009;66(3):245-252. doi:10.1016/j.biopsych.2009.02.032

58. Sexton CE, Allan CL, Le Masurier M, et al. Magnetic resonance imaging in late-life depression: multimodal examination of network disruption. *Arch Gen Psychiatry*. 2012;69(7):680-689. doi:10.1001/archgenpsychiatry.2011.1862

59. Taylor WD, MacFall JR, Gerig G, Krishnan RR. Structural integrity of the uncinate fasciculus in geriatric depression: Relationship with age of onset. *Neuropsychiatr Dis Treat*. 2007;3(5):669-674.

60. Shen X, Reus LM, Cox SR, et al. Subcortical volume and white matter integrity abnormalities in major depressive disorder: findings from UK Biobank imaging data. *Sci Rep*. 2017;7(1):5547. doi:10.1038/s41598-017-05507-6

61. Alves GS, Karakaya T, Fußer F, et al. Association of microstructural white matter abnormalities with cognitive dysfunction in geriatric patients with major depression. *Psychiatry Res*. 2012;203(2-3):194-200. doi:10.1016/j.pscychresns.2011.12.006

62. Rhodes E, Insel PS, Butters MA, et al; Alzheimer's Disease Neuroimaging Initiative; ADNI Depression Project. ADNI Depression Project. the impact of amyloid burden and APOE on rates of cognitive impairment in late life depression. *J Alzheimers Dis*. 2021;80(3):991-1002. doi:10.3233/JAD-201089

63. Wilkins CH, Mathews J, Sheline YI. Late life depression with cognitive impairment: evaluation and treatment. *Clin Interv Aging*. 2009;4:51-57.

64. de Nooij L, Harris MA, Adams MJ, et al. Cognitive functioning and lifetime major depressive disorder in UK Biobank. *Eur Psychiatry*. 2020;63(1):e28. doi:10.1192/j.eurpsy.2020.24

65. Lee SN, Hong K-M, Seong YS, Kwak SJ. Ectopic overexpression of coiled-coil domain containing 110 delays G2/M Entry in U2-OS cells. *Dev Reprod*. 2020;24(2):101-111. doi:10.12717/DR.2020.24.2.101

66. Monji M, Nakatsura T, Senju S, et al. Identification of a novel human cancer/testis

antigen, KM-HN-1, recognized by cellular and humoral immune responses. *Clin Cancer Res*. 2004; 10(18 Pt 1):6047-6057. doi:10.1158/1078-0432.CCR-04-0475

67. Howard DM, Adams MJ, Clarke T-K, et al; 23andMe Research Team; Major Depressive Disorder Working Group of the Psychiatric Genomics Consortium. Genome-wide meta-analysis of depression identifies 102 independent variants and highlights the importance of the prefrontal brain regions. *Nat Neurosci*. 2019;22(3):343-352. doi:10.1038/s41593-018-0326-7

68. Wray NR, Ripke S, Mattheisen M, et al; eQTLGen; 23andMe; Major Depressive Disorder Working Group of the Psychiatric Genomics Consortium. Genome-wide association analyses identify 44 risk variants and refine the genetic architecture of major depression. *Nat Genet*. 2018;50(5):668-681. doi:10.1038/s41588-018-0090-3

69. Shen X, Howard DM, Adams MJ, et al; Major Depressive Disorder Working Group of the Psychiatric Genomics Consortium. A phenome-wide association and Mendelian Randomisation study of polygenic risk for depression in UK Biobank. *Nat Commun*. 2020;11(1): 2301. doi:10.1038/s41467-020-16022-0

70. Lim GY, Tam WW, Lu Y, Ho CS, Zhang MW, Ho RC. Prevalence of depression in the community from 30 countries between 1994 and 2014. *Sci Rep*. 2018;8(1):2861. doi:10.1038/s41598-018-21243-x

71. Dönertaş HM, Fabian DK, Valenzuela MF, Partridge L, Thornton JM. Common genetic associations between age-related diseases. *Nat Aging*. 2021;1(4):400-412. doi:10.1038/s43587-021-00051-5

72. Corfield EC, Yang Y, Martin NG, Nyholt DR. A continuum of genetic liability for minor and major depression. *Transl Psychiatry*. 2017;7(5):e1131-e1131. doi:10.1038/tp.2017.99

73. Kida J, Nemoto K, Ikejima C, et al. Impact of depressive symptoms on conversion from mild cognitive impairment subtypes to alzheimer's disease: a community-based longitudinal study. *J Alzheimers Dis*. 2016;51(2):405-415. doi:10.3233/JAD-150603

74. Ownby RL, Crocco E, Acevedo A, John V, Loewenstein D. Depression and risk for Alzheimer disease: systematic review, meta-analysis, and metaregression analysis. *Arch Gen Psychiatry*. 2006;63(5):530-538. doi:10.1001/archpsyc.63.5.530

75. Jack CR, Knopman DS, Jagust WJ, et al. Update on hypothetical model of Alzheimer's disease biomarkers. *Lancet Neurol*. 2013;12(2):207-216. doi:10.1016/S1474-4422(12)70291-0